Avrami's law based kinetic modeling of colonization of mortar surface by alga Klebsormidium flaccidum

Thu Hien Tran, Alexandre Govin, René Guyonnet, Philippe Grosseau,
Christine Lors, Denis Damidot, Olivier Devès, Bertrand Ruot

Avrami's law based kinetic modeling of colonization of mortar surface by alga
Klebsormidium flaccidum

Thu Hien TRAN[a,b,c], Alexandre GOVIN[a], René GUYONNET[a], Philippe GROSSEAU[a], Christine LORS[b,c], Denis DAMIDOT[b,c], Olivier DEVES[d], Bertrand RUOT[d]

[a] : Ecole Nationale Supérieure des Mines de Saint Etienne, SPIN-EMSE, CNRS:UMR5307, PROPICE, LGF, 158 cours Fauriel, F-42023 St-Etienne, France
[b] : Université Lille Nord de France, 1 bis Georges Lefèvre, F-59044 Lille, France
[c] : Ecole Nationale Supérieure des Mines de Douai, LGCgE-GCE, 941 Rue Charles Bourseul, F-59508 Douai, France
[d] : Université Paris Est, Centre Scientifique et Technique du Bâtiment, Département Enveloppe et Revêtements, 84 avenue Jean Jaurès, Champs-sur-Marne,
F-77447 Marne-la-Vallée, France

Nomenclature

$X(t)$	colonization rate (%)
t	time (day)
t_l	latency time (day)
γ	number of algal spots at time t per unit area
$d\gamma/dt$	specific attachment rate (Spot/μm^2.day)
S	surface of an algal spot (μm^2)
k_g	specific attachment constant (Spot/μm^2.day^2)
k_c	growth rate constant (μm/day)
K	overall rate constant (Spot/day^4)
n	Avrami's exponent

Abstract

The aim of this research was to modelize the colonization of mortar surface by green algae using Avrami's law. The resistance of mortars, with different intrinsic characteristics (porosity, roughness, carbonation state), to the biofouling was studied by means of an accelerated lab-scale test. A suspension of green alga *Klebsormidium flaccidum*, was performed to periodically sprinkle the mortar surfaces. The covered surface rate followed a sigmoidal type curve versus time. Moreover, in order to apply Avrami's law, the algal colonization has been described by two processes: attachment and growth of algal cells. The image analysis showed that both the roughness and the carbonation influenced the algal attachment, unlike the porosity. The attachment specific rate increased linearly with time. For the algal growth process, it's difficult to conclude on the influence of mortar characteristics due to a high dispersion of experimental results. However, the assumption of a constant growth rate was acceptable. A good agreement between the simulation and the experimental results was obtained.

Keywords: modeling, Avrami's law, biological colonization, algae, mortar

1. Introduction

The building facades, after construction, are inevitably subject to the colonization by microorganisms which can induce an aesthetical degradation of the construction. These microorganisms may be bacteria, algae, cyanobacteria, fungi, lichens and even higher plants if no prevention is achieved. It is found that, except ubiquitous bacteria, algae are the first colonizers. Moreover, the *Klebsormidium flaccidum* algae are well known for their wide distribution (John 1988 ; Ortega-Calvo et al. 1991 ; Ortega-Calvo et al. 1993 ; Gaylarde and Gaylarde 2000 ; 2005 ; Crispim et al. 2003 ; Rindi et al. 2008) and like being the dominant microorganism in biofilm composition (Barberousse et al. 2006). The biological biofouling causes an aesthetic problem and thus a significant economic loss due to the maintenance and the repair of the facades.

The implantation of microorganisms depends on various-origins parameters. Indeed, under temperate or tropical climate, the composition of a biofilm and the dominant species are respectively different (Crispim et al. 2003). According to several authors the microclimate (i.e. light, moisture) is an essential parameter which controls the nature and the growth of the microorganisms (John 1988 ; Ariño et al. 1997). The microclimate is influenced by the inclination, the orientation, the distance from ground and the exposure to the shadow of a building facade. The substrate characteristics, such as porosity, surface roughness, chemical composition and surface pH, are obviously important (Deruelle 1991 ; Ortega-Calvo et al. 1995 ; Tomaselli et al. 2000 ; Tran et al 2012). Several authors showed that the biological colonization is faster on a rough wall (Wee and Lee 1980 ; Pietrini et al. 1985 ; Joshi and Mukudan 1997 ; Tomaselli et al. 2000 ; Tran et al. 2012). According to these authors, the roughness promotes the attachment of biological cells by providing numerous asperities. Moreover, a high porosity increases the amount of water available to microorganisms and thus favors their development (Ohshima 1999 ; Prieto and Silva 2005 ; Miller et al. 2006 ; Miller et al. 2009). On the contrary, the settlement by algae is slowed down or inhibited if the surface pH is greater than 11 (Grant 1982).

Several studies focused on the influence of these parameters on biofouling, at laboratory scale as well as at real scale. However, to our knowledge, very few studies have attempted to model this phenomenon. Ruot and Barberousse (2007) proposed a simulation of the surface materials colonization by algae. They showed that the Avrami's equation was quite a good tool to express the temporal evolution of the colonization rates. However, their study remains still preliminary and does not allow explaining the kinetic process and the role of material intrinsic characteristics.

Avrami's law, in the form of an exponential equation, has been developed by Avrami, Johnson and Melh for over 70 years (Avrami 1939 ; 1940 ; 1941 ; Johnson and Mehl 1939). This law was originally intended to describe the allotropic phase transformation in solids. Nowadays, it is used in many domains: crystallization of polymers, heat treatment in industry and thermal decomposition of solids ... (Hay 1971; Slovácek 2004). Avrami's model is based on two processes: the nucleation and the growth. The nucleation corresponds to the appearance of nuclei of a new phase. The growth represents the increase in the size of these nuclei into the initial phase during time.

In the case of this work, the fouling is initiated by the attachment of algae on the surface of the samples which creates many spots. The colonization rate follows a sigmoidal curve for the surface fraction colonized as function of time. As a consequence, colonization can be simulated thanks to the Avrami's model considering the algal spots as nuclei. Indeed, the algal spots are very small and randomly distributed on the surface. The extension of the fouling results from the increase in the size of the first algal spots by the growth of algal filament and from the adhesion of new spots as a function of time.

99   The aim of this study is to modelize the colonization mechanism of the surface materials
100   by algae using Avrami's model.
101
102
103   **2. Materials and methods**
104
105   The studied materials were mortars made up of Portland cement CEM I 52.5 N (Holcim),
106   siliceous sand (Sibelco DU 0.1/0.35) and calcareous filler (Omya). Table 1 gives the
107   proportions of each constituent. The mortar was prepared with a water to cement ratio w/c
108   (wt./wt.) of 0.5. In order to obtain a more porous mortar, the w/c ratio was increased to 1.
109   However, cellulose ether (Hydroxylethyl Methyl Cellulose - HEMC) was added as admixture
110   to thicken the mortar and thus avoiding segregation.
111
112   For each mortar, three finishing methods were applied on the surface of samples during
113   the setting. One corresponded to a smoothing by a ruler and the two other to a scratching by
114   sponges of two different roughnesses.
115
116   The mortar mixture was cast into $50 \times 50 \times 1$ cm expanded polystyrene moulds and
117   stored at 21 ± 1 °C and 95 ± 5 % of relative humidity (RH) during 28 days (for the
118   preparation of uncarbonated mortars). To prepare carbonated samples, the mortars were stored
119   only 7 days before being cut into $20 \times 8 \times 1$ cm samples. These samples were then stored in a
120   chamber under pure CO_2, at 21 ± 1 °C, and 65 ± 5 % relative humidity during 36 days.
121
122   The total porosity of materials was determined by mercury intrusion porosimetry
123   (Micromeritics Autopore IV 9400). For each mortar, three samples beforehand dried by
124   acetone were analyzed.
125
126   The surface roughness was measured using a CHR-150-L profilometer and was evaluated
127   by the arithmetic average of the height (R_a) (Gadelmawla et al. 2002).
128   The surface pH of mortars was measured by a surface electrode (WTW Sentix Sur). To
129   ensure contact between the substrate and the pH-electrode, a drop of water was deposed on
130   the surface before measurement.
131
132   The studied algal specie was *Klebsormidium flaccidum*. It was chosen due to its
133   representativeness and its facility of cultivation.
134
135   The bio-receptivity of mortar, depending on its characteristics (porosity, roughness,
136   carbonation state), was examined through a laboratory accelerated test. The experimental
137   device consisted of a $100 \times 50 \times 50$ cm closed glass chamber placed in a dark room. At the
138   beginning of the experiments, 50 L of sterilized Bold's Basal Medium (BBM) (Barberousse
139   2006) were inoculated with *K. flaccidum* in order to obtain an algal suspension of 4 mg.L^{-1} of
140   dry mass. The algal growth was carried out at 24 °C by means of a thermo-regulator. In this
141   device, two rows of samples were placed back to back on a stainless steel support inclined at
142   45°. Each row of samples was equipped with a system constituted of a stainless steel tube (10
143   mm diameter drilled every 10 mm) and two pumps (Rena Flow 650 BF). This device allowed
144   to the algal suspension, to flow on the top of each sample.
145   The sprinkling period and the flow rate were set respectively at 90 min every 12 h and at
146   26 ± 2 L.h^{-1}. The light was provided by two neon lamps (OSRAM Fluora L30W/77). The
147   photoperiod was of 12 h and was starting with the beginning of a sprinkling cycle.
148

149   In each test, 18 samples of materials were placed into the chamber. Each formulation was
150   tested in triplicates. Carbonated or uncarbonated samples were tested separately.
151   Table 2 gives the characteristics of the studied mortars. Each mortar was labeled
152   according to three codes. The first one was the w/c ratio (0.5 or 1), the second one expressed
153   the carbonation state (C for carbonated and UC for uncarbonated) and the third one
154   corresponded to the roughness (R1, R2 and R3). For example, a sample labeled 10C-R2
155   corresponded to a carbonated sample, carried out with a w/c ratio equal to 1 and with the
156   intermediate roughness.
157   To evaluate biofouling, the sample surface was daily digitized by means of an office
158   scanner. The area colonized by algae was determined by image analysis using Aphelion®
159   software. The colonization rate was given by the ratio of the colonized area to the total surface
160   and was noted X(t).
161   Full details of the experimental approach were described in a previous paper (Tran et al.
162   2012).
163   In order to experimentally determine the specific attachment rate and the growth rate of
164   algae, an algorithm was developed with Aphelion® software. The objective of the algorithm
165   was to quantify new spots appearing between time t and t+Δt by comparison of the two
166   images acquired respectively at time t and t+Δt. The growth rate was determined by following
167   the increase in the surface of each spot over time.
168
169
170   **3. Theoretical basis of the model**
171
172   An example of biodeterioration result is shown on Fig. 1a. On this figure, the effect of the
173   roughness on the biofouling of mortars by algae is highlighted for the mortar serie 10C (10
174   and C mean a w/c equal to 1 and carbonated, respectively). In fact, whatever the mortars
175   studied, the shape of the curve, X(t), was always the same: sigmoidal type (Tran et al. 2012).
176   In all cases, three steps were identified: a latency step, an exponential growth step and a step
177   of stagnation (Tran et al. 2012). This type of curve can be well simulated by using Avrami's
178   equation (Ruot and Barberousse 2007). As mentioned in the introduction, the Avrami's law is
179   used to modelize the kinetics of allotropic phase transformations in solids. This model is
180   based on two processes: the nucleation and the growth of nuclei. The nucleation corresponds
181   to the formation of nuclei of a new phase. The growth corresponds to the increase in the size
182   of these nuclei in the initial phase during time. However, the Avrami's law is only valid under
183   the four assumptions below:
184   –   the volume of the initial phase is unlimited compared to the nucleus one,
185   –   the nuclei must be distributed randomly in the volume of the solid,
186   –   the form and the growth of all the nuclei are identical,
187   –   the growth rate is independent of the appearance time of the nucleus.
188
189   According to our biofouling results, an analogy between a chemical transformation and
190   the fouling can be drawn. Thus it allows applying Avrami's theory. Indeed, during an
191   allotropic transformation, the old phase is transformed into new one. In the case of the
192   biological fouling of mortars, it is possible to consider the uncolonized mortar as the old
193   phase and the mortar colonized by algae (algae attached on the surface of the mortar) as the
194   new phase. In both cases, the transformation of the old phase into new one results from the
195   displacement of the interface between both phases. Moreover, if we consider the algal
196   biofouling of mortars, the curves dX/dt=f(X), such as those in Fig. 1b, exhibit a maximum. In
197   the case of chemical reaction, such as thermal decomposition of solid, it suggests that the
198   reaction involves simultaneous nucleation and growth processes of the new phase (Galwey

4

and Brown). Kinetics modeling of these reactions are usually done using a general expression of the reaction rate under the form dX/dt=A.f(X). A is a preexponential factor, which depends on temperature and activation energy and f(X) a function of the fractional conversion X. When X(t) is a sigmoidal curve, authors often use the Avrami laws to express f(X). As it is shown on fig. 1a, in our case, the colonization rate X(t) corresponds to a sigmoidal curve.

Moreover, the sample fouling is initiated by the attachment of algae on the surface of the samples. It results in the appearance of very small green spots on the surface, corresponding to algae, which can be assimilated to nuclei in the Avrami's model. The smaller algal spot detected by image analysis, i.e. one pixel, was about 7200 μm^2. This surface is very small compared to the samples size (160 10^8 μm^2). Thus the sample may be considered as infinite, as required by a two-dimensional Avrami's model. The thickness of algae biofilm was not investigated here.

The extension of the fouling results from the growth of the first algal spots and from the adhesion of new ones (Fig. 2). This confirms that the attachment and the growth occurred simultaneously, which allows the use of Avrami's model.

In addition, the algal spots appeared randomly on the sample surface as required by the Avrami's model.

Thus, the colonization by algae has been considered as the combination of two processes: the attachment and growth of algal spots, which were assimilated respectively to the "nucleation" step and to the growth step of the "nuclei" described in the Avrami's model.

To simplify the modeling, it was assumed that the attachment ("nucleation" in the Avrami's model) occurred with the same probability over the entire surface of the sample. As a consequence, the surface defects, such as air bubbles, did not affect the attachment of algae.

Fig. 1 showed that no colonization of the sample surfaces by algae occurred during several days. This time was called latency period. During this period the attachment and the growth of algae were null. The duration of this phase can depend on several parameters, such as sprinkling period, chemical composition of the specimen and of the culture medium... The latency time (t_l) was defined as the time corresponding to a colonization rate of 0.5 %. The best reproducibility was obtained using this method.

In general, the attachment and the growth of algae on the mortar surface might be affected by the porosity (p), the roughness (R), the initial pH of the surface (pH), the chemical composition of the mortar, the algae species, the algae viability, the light intensity, the temperature, the inclination of the substrate surface and the sprinkling flow. However, except the material properties (porosity, roughness and surface pH), all other experimental parameters were constantly fixed.

The specific attachment rate was defined as the number of algal spots appearing on surface unit per time unit (eq.1).

$$\frac{d\gamma}{dt} = k_g(p, R, pH) \times (t - t_l)^q \qquad (1)$$

Where:
γ is the number of algal spots at time t per unit area (Spot/μm^2).
k_g is the attachment specific rate constant (Spot/μm^2.day^{q+1}).
t_l corresponds to the latency time (day).

Concerning the growth, the hypotheses that the growth rate was identical for all algal spots and was constant during time were applied. The surface area covered by an algal spot appearing at time θ was expressed as follow:

$$s_g(t,\theta) = k_c^2(t-\theta)^2 \tag{2}$$

Where k_c corresponds to the specific growth rate constant (µm/day).

k_c takes into account the growth rate in each direction (x and y) and the form of the algal spot.

The colonization rate X(t) was calculated from the law of "nucleation" and growth previously expressed, as an exponential equation (eq. 3) (Delmon 1969).

$$X(t) = 1 - e^{-K(t-t_1)^n} \tag{3}$$

Where:

$$K = A k_g k_c^2 \tag{4}$$

$$\text{with} \quad A = \frac{2}{(q+1)(q+2)(q+3)} \tag{5}$$

$$n = q+3 \tag{6}$$

4. Results

4.1. Experimental examination of algal attachment process

The determination of the specific attachment rate of algae was carried out by the algorithm developed with Aphelion software. At each time step, new algal spots fixed on the surface were counted by image analysis. The specific attachment rate was thus calculated for each material by dividing the number of new algal spots per unit of time by the initial sample surface. The size of the smallest algal spot which could be detected was approximately 85×85 µm (7200 µm^2). It corresponded to around 80 times the surface of an algal cell but only 4.5×10^{-7} times the sample surface. This justified the hypothesis that the surface of the sample could be considered as infinite as required by the Avrami's model.

This process was applied only in the early stage where less than 8 % of sample surface was covered by algae. A more advanced colonization disrupted the fixation of new algal cells and therefore distorted the determination of the specific attachment rate constant (k_g).

4.1.1 Influence of mortar characteristics on the algal attachment process

Fig. 3 illustrates the evolution, during time, of the specific attachment rate of algae for carbonated mortars mixed with a w/c ratio of 1. For each samples, the specific attachment rate is null during several days. This result confirms the existence of a latency period during which no spot is fixed to the surface. Moreover, despite important uncertainties, influence of the roughness on the algal attachment rate is obvious. Indeed, the rougher the mortar is, the higher the attachment rate is.

The effect of the carbonation of mortars (roughness R2 and w/c = 1), on the algal attachment rate is shown on Fig. 4. The attachment rate reached for the uncarbonated mortar is much smaller than for the carbonated one.

293   For carbonated mortars and roughness R2, the influence of w/c ratio on the attachment
294   rate is illustrated on Fig. 5. The results demonstrate that attachment specific rate for w/c ratios
295   of 0.5 and 1 are very close. Thus, in our study, the effect of the porosity was negligible on the
296   biofouling.
297
298   4.1.2 Specific attachment rate constant
299

300   According to the Figs. 3, 4 and 5, beyond the latency time, the specific attachment rate,
301   which is equivalent to the "nucleation" rate in the Avrami's model, increases linearly with
302   time. This result implies that the specific attachment rate can be modelized by a power law. In
303   this case, the value of the power (q) is equal to 1 to express the attachment rate. Thus the
304   specific attachment constant (k_g) can be determined, beyond the latency time (t_l), by a linear
305   regression. Fig. 3 illustrates the fit obtained for carbonated mortars with a w/c ratio equal to 1.
306   The values of k_g for all the studied mortars are summarized in Table 3. For all the
307   samples, to the exception of 05R3-C, k_g is strongly dependent of the roughness. Indeed, when
308   the roughness increases, k_g also increases. For example, k_g of carbonated samples is 9 times
309   higher and 30 times higher when the roughness increases from R1 to R2 and from R1 to R3
310   respectively.
311   The behavior of the 05R3-C sample for which the specific attachment constant was
312   smaller than the one obtained for 05R2-C was particular. Despite a high R_a value (186µm),
313   the micro-roughness created by the sand grains was missing from the surface of these
314   samples. This micro-roughness is important in promoting the algal adherence.
315   Moreover, beyond a roughness of 30µm, the relationship between k_g and the roughness
316   (R_a) seems to be linear (Fig. 6a). The slope of the straight line is around 4.6 and 0.7
317   respectively for the carbonated samples and the uncarbonated ones. So the carbonated
318   samples are more sensitive to the roughness than uncarbonated ones.
319   In addition, the carbonation, and then the surface pH, impacts the specific attachment
320   constant. Indeed, whatever the roughness, k_g is always higher for carbonated samples than for
321   uncarbonated ones.
322
323   4.1.3 Latency time
324

325   The values of t_l are summarized in Table 3. The latency time decreased with the roughness
326   and the carbonation. For carbonated samples, the effect of the roughness is weak (fig. 6b).
327   However, the effect is strongly marked with uncarbonated mortars.
328   Moreover, the latency time is really dependent of the chemical state of the surface. Indeed,
329   the carbonation of the mortars decreases the latency time and thus increases the
330   biocompatibility of the substrate. For example, the latency times range from 6 to 10 days for
331   carbonated samples and from 17 to 44 days for uncarbonated ones.
332
333   **4.2.**   **Experimental examination of growth process**
334

335   Image analysis and specific algorithm enabled us to locate and track changes, during
336   time, of the surface of each algal spot found on the surface of the sample. The evolution of the
337   spot surface corresponds to the growth of algae and thus to a growth rate.
338   The growth rate constant (k_c) was experimentally determined and calculated according to
339   the equation (7).
340

341
$$k_c = \frac{\sqrt{S_{t+\Delta t}} - \sqrt{S_t}}{((t + \Delta t) - t)} \qquad (7)$$

342
343   Where:
344   S_t represents the area of an algal spot at time t (μm^2)
345     $S_{t+\Delta t}$ represents the area of the same algal spot at time t+Δt (μm^2)
346
347   Fig. 7 shows the evolution of k_c with time for carbonated samples of w/c ratio equal to
348   0.5. The values of k_c were determined for colonization rates below 50 %. Beyond this value,
349   the number of algal spots that could be isolated to monitor their growth became too low. By
350   considering the high dispersion of experimental results, the growth rate constant (k_c) does not
351   seem to vary significantly with time. This remark is also valid for all other mortars.
352   If the growth rate constant is considered as independent of time, the average of this
353   constant could be calculated for each material. The results are presented on Fig. 8.
354   Experimental errors were very important. It is therefore difficult to highlight the effect of
355   intrinsic characteristics of materials on the growth rate constant. However, despite these
356   uncertainties, it seems that, for each type of sample, the algal growth was lower on the
357   uncarbonated samples than on the carbonated ones.
358
359   **4.3.   Simulation of colonization rates**
360
361   In order to simulate the colonization process and in accordance with the results of
362   paragraph 4.1.2, q was fixed to 1 and thus n was equal to 4. The K parameter was adjusted
363   from the equation (3) by the least squares method (K was determined so that the error was
364   minimal). In order to express the deviation between the model and experimental data, a
365   fiability factor (R) was calculated as follow:
366

$$R = \sqrt{\frac{\sum_{t=1}^{m}(X_{st} - X_{et})^2}{\sum_{t=1}^{m}X_{et}^{\,2}}} \tag{8}$$

367
368
369   Where:
370   X_{st} represents the simulated colonization rate at time t
371   X_{et} represents the experimental colonization rate at time t
372
373   All the values of K are summarized in the Table 3. As expected, K increases with the
374   roughness and the carbonation with the exception of sample 05C-R3 (w/c=0.5, carbonated
375   and high roughness). This result was previously described and discussed in paragraph 4.1.2.
376   By using the equation (3) and the values of K, it was possible to simulate the colonization
377   rate. For all the carbonated mortars, the simulated curves were close to the experimental
378   points (Fig. 9). The fiability factors were small with a maximum error lower than 11 %. For
379   most of the uncarbonated mortars, a good agreement between simulated colonization rate and
380   experimental data was obtained (Fig. 10). However, divergences can be noticed for the 10UC-
381   R2 serie (w/c=1, uncarbonated and intermediate roughness) which was not well simulated.
382   Indeed, the fiability factor is equal to 25%. However, as shown on fig. 10, these mortars
383   exhibited abnormal behavior in our experiments.
384
385   **4.4.   Comparison between the experimental and the calculated growth rate**
386   **constant**
387

388   From the experimental values of k_g determined by image analysis, the values of the
389   growth rate constant ($k_{c\text{-calculated}}$) were calculated by the equation (9). Results obtained were
390   compared with those experimentally determined.
391

392
$$k_{c-calculated} = \sqrt{\frac{K}{Ak_g}} \qquad (9)$$

393

394   As shown in Fig. 11, for all mortars, calculated values were higher than experimental
395   ones. Except in the case of mortar 05UC-R1, for which the calculated value reached up 4
396   times the experimental one, the ratios between $k_{c\text{-calculated}}$ and $k_{c\text{-experimental}}$ were inferior to 3 for
397   all the cases. Taking into account the uncertainties, the two values remained nevertheless
398   close.
399

5. Discussion

401

402   In this paper, it was demonstrated that the Avrami's theory could be applied in order to
403   simulate the colonization kinetic of mortar surfaces by algae, in an accelerated laboratory test.
404   For almost all mortars, the simulated curves are very close to the experimental results. The
405   nucleation-growth mechanism is well adapted to describe the phenomenon of biological
406   colonization. Indeed, the colonization started by attachment of small algal spots (called
407   "nuclei" in Avrami's law) and is extended by the growth of these latter. Each of these two
408   processes was directly analyzed by image analysis.
409   The algal attachment on a surface is particularly complex, depending on several
410   parameters such as the microorganism nature, the substrate type, the medium type, the
411   microorganism concentration, which modify the interactions between the substrate and
412   microorganisms and microorganisms themselves. However, in the case of this work, the
413   mechanism of attachment was not studied. The author focused on the macroscopic aspect of
414   the algal adhesion. Indeed, the size of the smallest area of algal spot which could be detected
415   by image analysis was approximately 7200 μm^2. This area corresponded to around 80 times
416   the surface of an algal cell. So, a spot is composed of a lot of algal cells. This spot concept
417   integrates the complex phenomena involved in the adhesion of cells to a surface, the cell
418   density and the surface properties which depend on metabolic activity and physiological state,
419   necessary to retention and self-organization of cells (Carnazza et al. 2011).
420

421   The algal attachment on the sample surface was significantly influenced by the
422   roughness. Indeed, roughness provides asperities, which promoted the anchorage of algal
423   cells. It results in a higher specific attachment rate and a shorter latency time.
424   The carbonation, by decreasing surface pH, favored the attachment and growth processes.
425   It produced the same effects than the roughness, i.e. increasing the specific attachment rate
426   and shortening the latency time. However, unlike the roughness which acts physically on the
427   ability of algae to cling on a substrate, the carbonation may affect the algal metabolism.
428   Indeed, in the case of carbonated mortars, the algal cells are in a less alkaline medium, and so,
429   less stressful conditions than in the case of uncarbonated ones. The ability of attaching and
430   spreading of algae on the surface are thus better for carbonated samples (Tran et al. 2012).
431   The growth of the spots is the consequence of the vegetative or cellular multiplication which
432   is favored at low pH (Škaloud, 2006).
433

434   The attachment of algae on the surface of the substrate is governed by adaptive metabolic
435   interactions between algal cells and the substrate (Fattom et Shilo 1984, Finlay et al. 2002,

9

Barberousse 2006). The algal extracellular polysaccharides can play the role of glue (Robins et al. 1986, Gantar et al. 1995, Barberousse 2006). These polymers are involved in the initial contact between the cell and the surface, and act over time (Barberousse 2006). Indeed, they exist permanently on the cell wall and are adsorbed on the surface in contact.

These metabolites are composed of hexoses (glucose, galactose, mannose), 6-deoxyhexoses (rhamnose, fucose) and pentoses (xylose, arabinose). The main constituent depends on the algal species considered and the substrate. For *Klebsormidium flaccidum*, mannose was identified as the major component (Barbarosse 2006).

In contrast, the role of w/c ratio on the algal attachment was not detected. As mentioned by Tran et al. (2012), due to the test conditions, the mortars permanently contained abundant water. So this last was not a limited factor for the algal growth.

It was proved by image analysis that, in the early stage, algal specific attachment rate evolved linearly with time. In order to model the colonization rate (eq. (3)), it was supposed that the attachment rate increased linearly with time, throughout all the process.

The influence of intrinsic material characteristics on the growth process has not been shown due to important experimental uncertainties. The errors may result from the detachment of ancient cells or the adherence of new cells at the periphery of existing spots due to the periodic runoff. In these cases, the surface variation of spots was no longer only related to their growth. However, the assumption of constant growth rate over time was found acceptable.

The variation in algal activity between the different tests prevents us from generalizing the results. Thus, no general equation describing the relationship between the kinetic parameters (t_l, k_g) and the intrinsic material parameters could be obtained.

6. Conclusion

The kinetic of biological colonization on mortar surface was well modelized in applying Avrami's theory. The experimental conditions used in this study were suitable for the application of the Avrami's model and satisfied to assumptions of the model. The model based on two steps, "nucleation" or attachment and growth, closely represents the colonization rate.

The influence of roughness and carbonation on the attachment frequency was highlighted. These two intrinsic parameters promoted the anchorage of algae on the substrate by increasing the attachment rate and by shortening the latency time. The porosity had no effect in our tests.

According to the results, the evolution of the attachment rate as function of time seems linear. So the attachment rate followed a powerful law with a power q equal to 1.

Due to large experimental uncertainties, it was difficult to conclude on the growth rate of algal spots. However, supposition of a constant growth rate of spots appeared acceptable.

References

Ariño, X., Gomez-Bolea, A., Saiz-Jimenez, C., 1997. Lichens on ancient mortar. International Biodeterioration and Biodegradation 40, 217-224.

Avrami, M., 1939. Kinetics of phase change I - General Theory. Journal of Chemical Physics 7, 1103-1112.

Avrami, M., 1940. Kinetics of phase change II - Transformation-Time Relations for Random Distribution Nuclei. Journal of Chemical Physics 8, 212-224.

486	Avrami, M., 1941. Granulation, phase change, and microstructure - Kinetics of phase
487	change III. Journal of Chemical Physics 9, 177-185.
488	Barberousse, H., Tell, G., Yéprémian, C., Couté, A., 2006. Diversity of algae and
489	cyanobacteria growing on building façades in France. Algological Studies 120: 83-110.
490	Carnazza, S., Marletta, G., Frasca, M., Fortuna, L., Guglielmino, S., 2011. Spatial
491	patterns of microbial retention on polymer surfaces. Journal of Adhesion Science and
492	Technology 25, 2255-2280
493	Crispim, C.A., Gaylarde, P.M., Gaylarde, C.C., 2003. Algal and cyanobacterial biofilms
494	on calcareous historic buildings. Current Microbiology 46, 79-82.
495	Delmon, B., 1969. Introduction à la cinétique hétérogène. Ed. Technip, Paris.
496	Deruelle, S., 1991. Rôle du support dans la croissance des microorganismes. Materials
497	and Structures 24, 163-168.
498	Fattom, A., Shilo, M., 1984. Hydrophobicity as an adhesion mechanism of benthic
499	cyanobacteria. Applied and Environmental Microbiology 47, 135-143.
500	Finlay, J.A., Callow, M.E., Ista, L.K., Lopez, G.P., Callow, J.A., 2002. The Influence of
501	Surface Wettability on the Adhesion Strength of Settled Spores of the Green Alga
502	Enteromorpha and the Diatom Amphora. Integrative and Comparative Biology 42, 1116-
503	1122.
504	Galwey, A.K., Brown, M.E., 1999 Thermal Decomposition of Ionic Solids, Elsevier,
505	Netherlands.
506	Gantar, M., Rowell, P., Kerby, N.W., 1995. Role of extra- cellular polysaccharides in the
507	colonization of wheat (Triticum vulgarie L.) roots by N_2-fixing cyanobacteria. Biology and
508	Fertility of Soils 19, 41-48.
509	Gaylarde,P.M., Gaylarde, C.C., 2000. Algae and cyanobacteria on painted buildings in
510	Latin America. International Biodeterioration and Biodegradation 46, 93-97.
511	Gaylarde, C.C., Gaylarde, P.M., 2005. A comparative study of the major microbial
512	biomass of biofilms on exteriors of buildings in Europe and Latin America. International
513	Biodeterioration and Biodegradation 55, 131-139.
514	Grant, C., 1982. Fouling of terrestrial substrates by algae and implications for control – a
515	review. International Biodeterioration Bulletin 18, 57-65.
516	Hay, J. N., 1971. Application of the modified avrami equations to polymer crystallisation
517	kinetics. British Polymer Journal 3, 74–82.
518	John, D.M., 1988. Algal growth on buildings: A general review and methods of
519	treatment. Biodeterioration Abstracts 2, 81-102.
520	Joshi, C.D., Mukunda, U., 1997. Algal disfigurement and degradation of architectural
521	paints in India. Paintindia 47, 27-32.
522	Johnson, W.A., Mehl, R.F., 1939. Reaction Kinetics in Processes of Nucleation and
523	Growth. Trans. Amer. Inst. Ming. Metall. 135, 416-458.
524	Miller, A., Dionísio, A., Macedo, M.F., 2006. Primary bioreceptivity: A comparative
525	study of different Portuguese lithotypes. International Biodeterioration and Biodegradation
526	57, 136-142.
527	Miller, A.Z., Dionísio, A., Laiz, L., Macedo, M.F., Saiz-Jimenez, C., 2009. The influence
528	of inherent properties of building limestones on their bioreceptivity to phototrophic
529	microorganisms. Annals of Microbiology 59, 705-713.
530	Ohshima, A., Matsui, I., Yuasa, N., Henmi, Y., 1999. A study on growth of fungus and
531	algae on mortar. Transactions of the Japan Concrete Institute 21, 173-178.
532	Ortega-Calvo, J.J., Hernandez-Marine, M., Saiz-Jimenez, C., 1991. Biodeterioration of
533	building materials by cyanobacteria and algae. International Biodeterioration 28, 165-185.

534   Ortega-Calvo, J.J., Sanchez-Castillo, P.M., Hernandez-Marine, M., Saiz-Jimenez, C.,
535 1993. Isolation and characterization of epilithic chlorophytes and cyanobacteria from two
536 Spanish cathedrals (Salamanca and Toledo). Nova Hedwigia 57, 239-253.

537   Ortega-Calvo, J.J., Ariño, X., Hernandez-Marine, M., Saiz-Jimenez, C., 1995. Factors
538 affecting the weathering and colonization of monuments by phototrophic microorganisms.
539 Science of The Total Environment 167, 329-341.

540   Pietrini, A.M., Ricci, M., Bartolini, M., Giuliani, M.R., 1985. A reddish colour alteration
541 caused by algae on stoneworks. Proceedings of the Vth international congress on deterioration
542 and conservation of stone, Presses polytechniques romandes, Lausanne, 653-662.

543   Prieto, B., Silva, B., 2005. Estimation of the potential bioreceptivity of granitic rocks
544 from their intrinsic properties. International Biodeterioration and Biodegradation 56, 206-215.

545   Rindi, F., Guiry, M.D., López-Bautista, J.M., 2008. Distribution, morphology, and
546 phylogeny of *Klebsormidium* (*Klebsormidiales, Charophyceae*) in urban environments in
547 Europe. Journal of Phycology 44, 1529-1540.

548   Robins, R.J., Hall, D.O., Shi, D.J., Turner, R.J., Rhodes, M.J.C., 1986. Mucilage acts to
549 adhere cyanobacteria and cultured plant cells to biological and inert surfaces. FEMS
550 Microbiology Letters 34, 155-160.

551   Ruot, B., Barberousse, H. (2007). Quantification and kinetic modeling of the colonisation
552 of façade rendering mortars by algae. VII SBTA, Recife, Brazil, 1-12.

553   Škaloud, P., 2006. Variation and taxonomic significance of some morphological features
554 in european strains of *Klebsormidium* (*Klebsormidiophyceae*, *Streptophyta*). Nova Hedwigia
555 83, 533-550.

556   Slovácek, M., 2004. Application of numerical simulation of heat treatment in industry. J.
557 Phys. IV France 120, 753-760.

558   Tomaselli, L., Lamenti, G., Bosco, M., Tiano, P., 2000. Biodiversity of photosynthetic
559 micro-organisms dwelling on stone monuments. International Biodeterioration and
560 Biodegradation 46, 251-258.

561   Tran, T.H., Govin, A., Guyonnet, R., Grosseau, P., Lors, C., Garcia-Diaz, E., Damidot,
562 D., Deves, O., Ruot, B., 2012. Influence of the intrinsic characteristics of mortars on
563 biofouling by *Klebsormidium flaccidum*. International Biodeterioration and Biodegradation
564 70, 31-39.

565   Wee, Y.C., Lee K.B., 1980. Proliferation of algae on surfaces of buildings in Singapore.
566 International Biodeterioration Bulletin 16, 113-117.

567
568

569

570 Table 1. Mortar formulation

571

Component	Cement	Sand	Calcareous Filler	Admixture[a] (in the case of w/c = 1)
% mass of dry mixture	30	65	5	0.27

572 [a] in addition to dry mixture (cement, sand and filler)

573

574

575

576 Table 2. Characteristics of the mortars

577

	Ratio w/c	Porosity (%)	Surface pH		Code	R_a (µm)
Carbonated	0.5	10.6 ± 0.4	9.5 ± 0.2	Roughness 1	05C-R1	40 ± 9
				Roughness 2	05C-R2	90 ± 8
				Roughness 3	05C-R3	186 ± 21
	1.0	32.1 ± 1.9	9.0 ± 0.1	Roughness 1	10C-R1	30 ± 3
				Roughness 2	10C-R2	55 ± 4
				Roughness 3	10C-R3	169 ± 17
Uncarbonated	0.5	15.9 ± 0.6	11.2 ± 0.4	Roughness 1	05UC-R1	29 ± 5
				Roughness 2	05UC-R2	47 ± 6
				Roughness 3	05UC-R3	123 ± 9
	1.0	37.2 ± 0	11 ± 0.4	Roughness 1	10UC-R1	29 ± 5
				Roughness 2	10UC-R2	55 ± 4
				Roughness 3	10UC-R3	123 ± 9

578

579

580

581 Table 3. Experimental and calculated kinetic parameters and fiability factor

582

	Mortar	t_l (day)	k_g (×10^{10}) (spot/µm^2.day^2)	$k_{c-experimental}$ (µm/day)	K (×10^6) (spot/day^4)	R (%)	$k_{c-calculated}$ (µm/day)
Carbonated	10C-R1	10 ± 2	21.3	184 ± 147	22.3	5	299
	10C-R2	8 ± 1	183.9	122 ± 93	193.6	7	350
	10C-R3	6 ± 1	652.6	109 ± 71	437.9	7	285
	05C-R1	9 ± 2	39.0	132 ± 103	36.2	11	337
	05C-R2	8 ± 1	376.2	101 ± 87	492.5	10	298
	05C-R3	8 ± 2	127.0	124 ± 95	76.4	8	263
Uncarbonated	10UC-R1	27 ± 1	1.5	74 ± 68	0.2	8	131
	10UC-R2	20 ± 1	84.1	66 ± 51	1.5	25	103
	10UC-R3	18 ± 2	86.3	83 ± 57	31.8	12	201
	05UC-R1	44 ± 5	1.9	60 ± 50	0.7	8	237
	05UC-R2	27 ± 4	8.4	74 ± 47	0.4	8	72

13

| | 05UC-R3 | 17 ± 3 | 66.1 | 83 ± 58 | 32.7 | 12 | 178 |

584

(a)

585

(b)

586
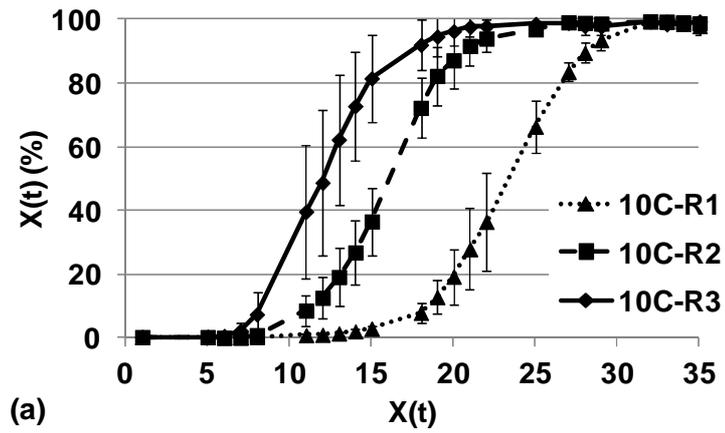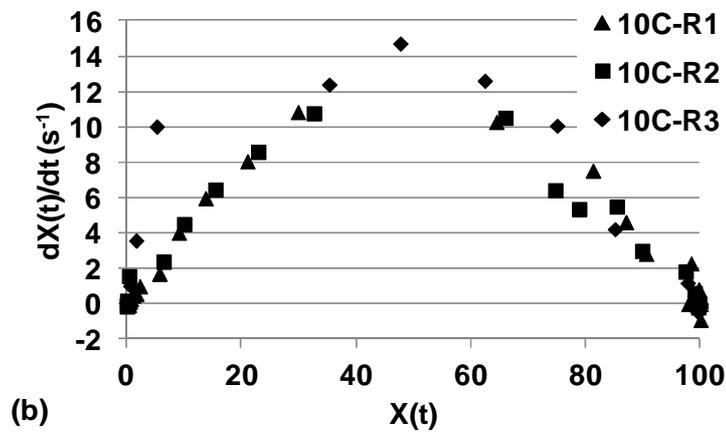
Fig. 1 Influence of roughness (R1=30µm, R2=55µm and R3=169µm) on the algal biofouling

of carbonated (C) mortars with a w/c ratio equal to 1: a) X(t) and b) dX(t)/dt

589

15

590

| 12 days | 19 days | 26 days |
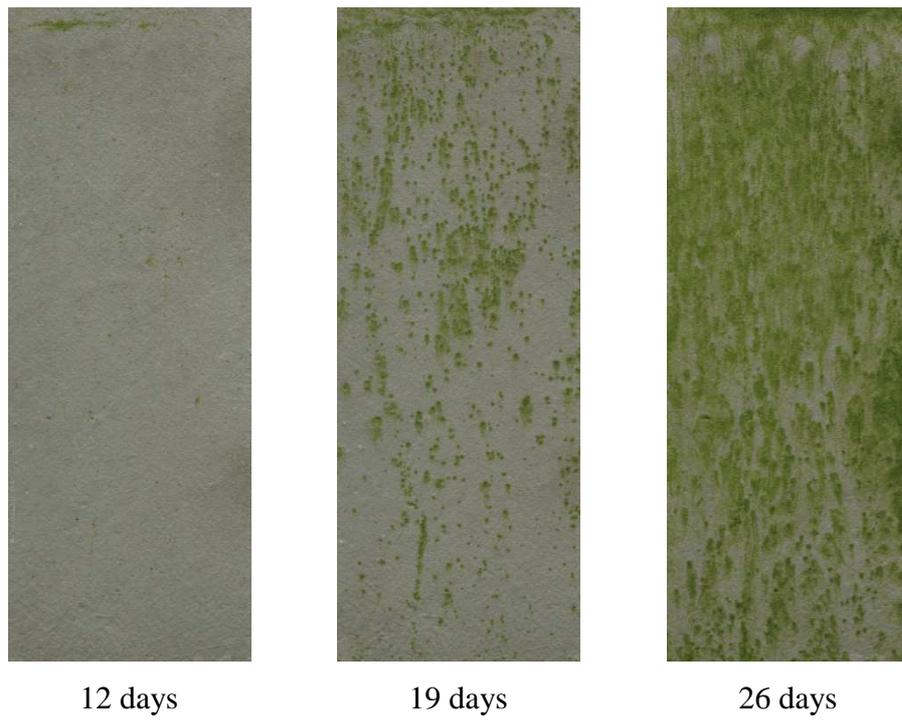
591   Fig. 2 Surface of carbonated mortars with a w/c ratio of 0.5 and a roughness R1, colonized by

592   algae over time

593

594
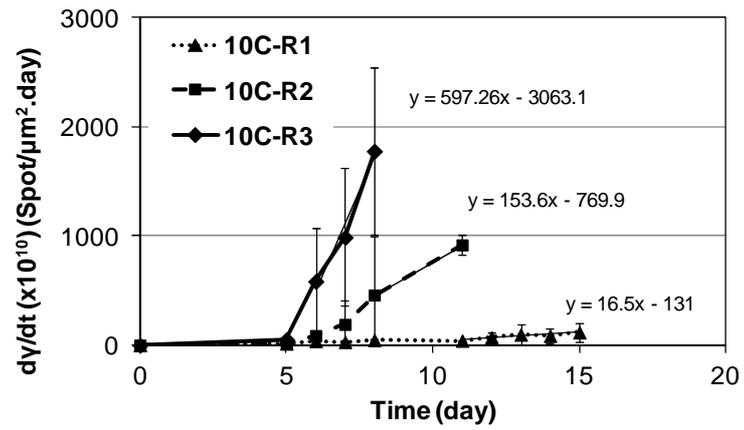
Fig. 3 Influence of the roughness (R1, R2 and R3) on the specific attachment rate of algae
(specifications of mortars: carbonated (C) and w/c ratio of 1)

595

596

597

598

599
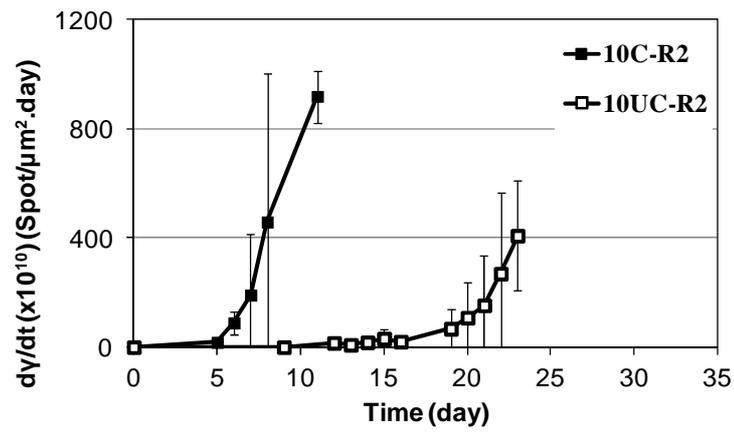
600

601   Fig. 4 Influence of the carbonation state (C for carbonated and UC for uncarbonated) on

602   the specific attachment rate of algae (specifications of mortars: intermediate roughness (R2),

603   w/c ratio of 1)

604

605
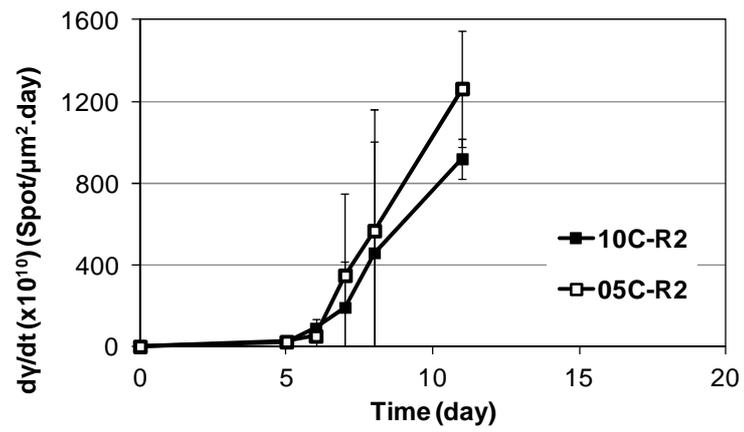
606

607   Fig. 5 Influence of the w/c ratio on the specific attachment rate of algae (specifications of

608   mortars: carbonated (C) and intermediate roughness (R2))

609

610
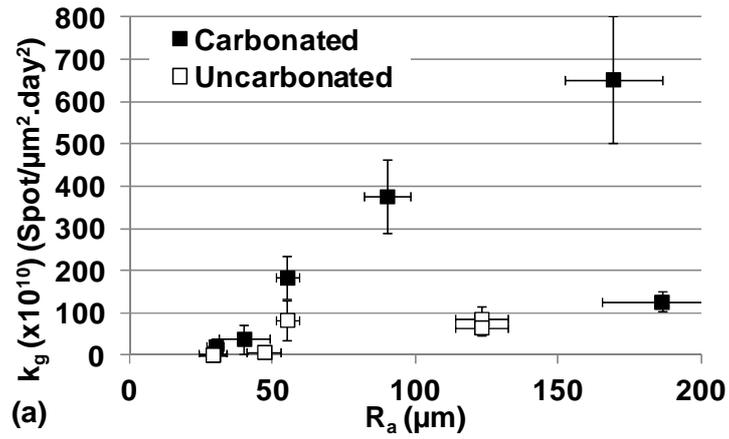
611
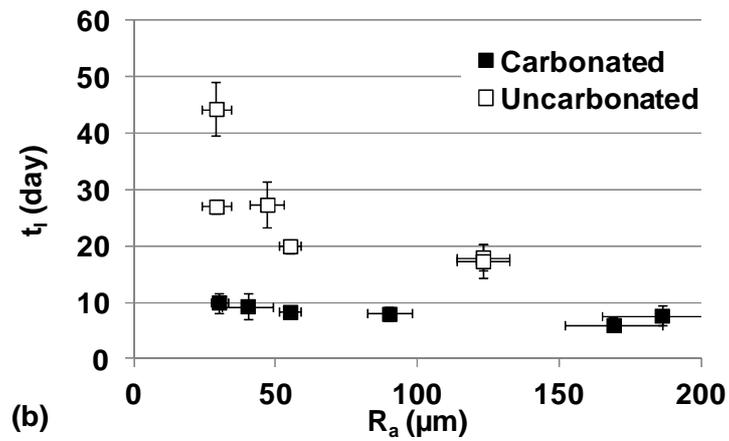
612
613   Fig. 6 Effect of roughness (R_a) on the specific attachment constant (a) and on the latency

614   time (b) for carbonated (C) and uncarbonated (UC) mortars

615

616
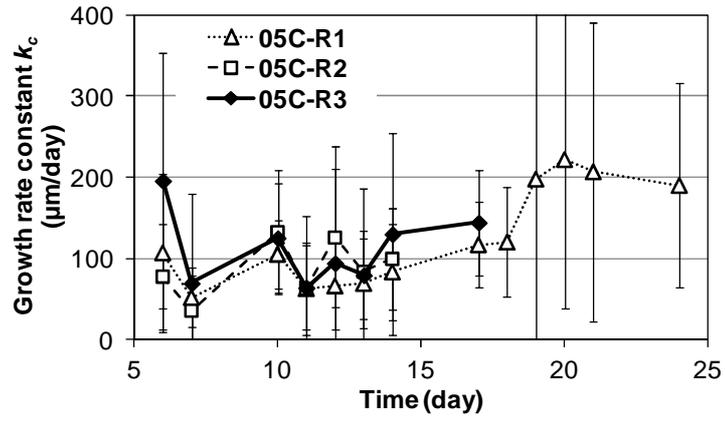
617

618   Fig. 7 Influence of roughness (R1, R2 and R3) on the growth rate constant versus time

619   (specifications of mortars: carbonated (C) and w/c ratio of 0.5)

620

621

622
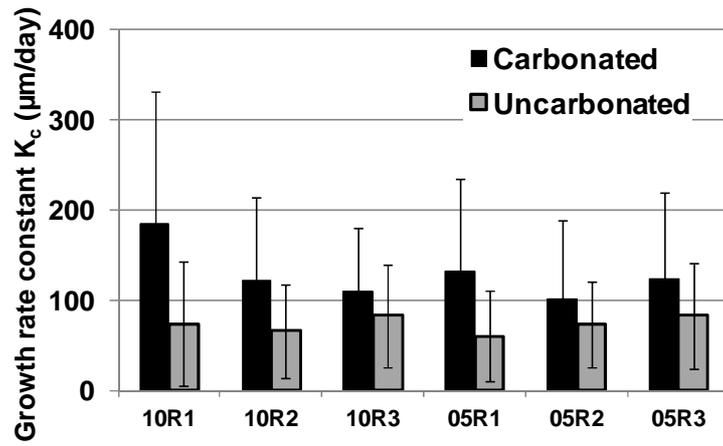
Fig. 8 Average of the growth rate constant for all the studied samples

623

624

625

626

627
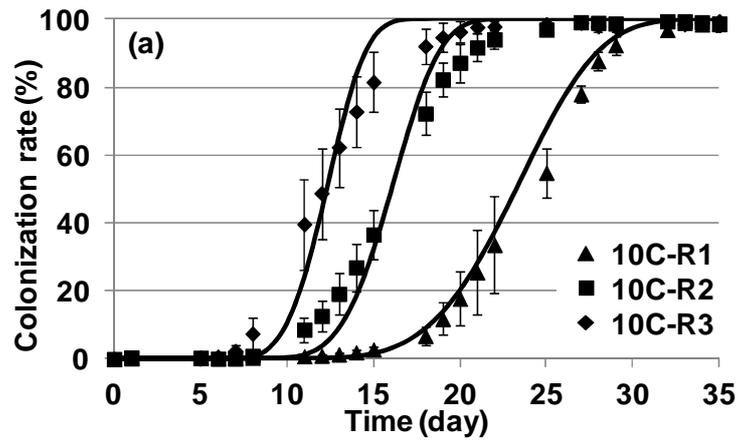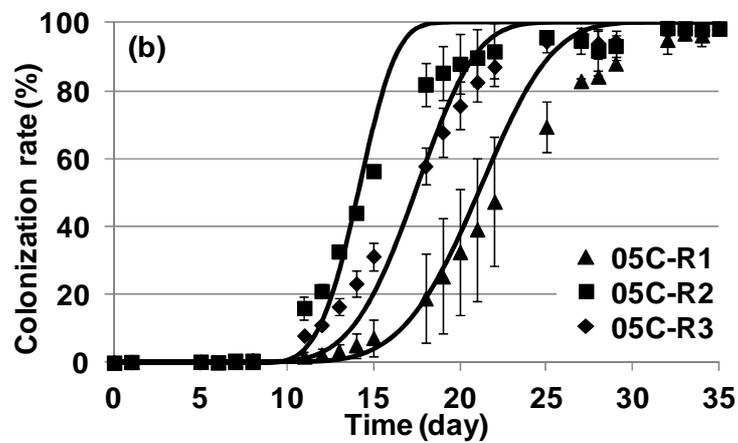
Fig. 9 Simulation of colonization rate for carbonated mortars mixed with w/c ratio of 1 (a) and

0.5 (b) (points: experimental data; lines: simulation)

630

631

632

633
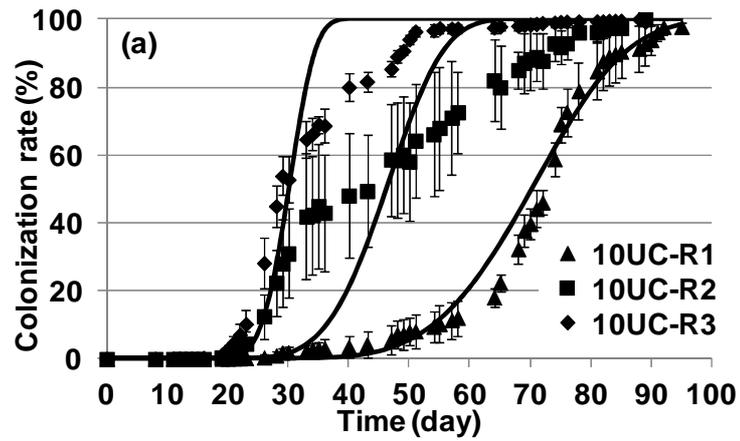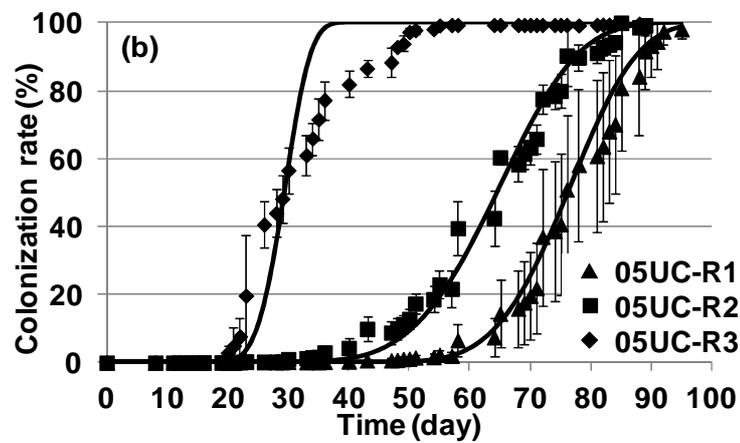
Fig. 10 Simulation of colonization rate for uncarbonated mortars mixed with w/c ratio of
1 (a) and 0.5 (b) (points: experimental data; lines: simulation)

636
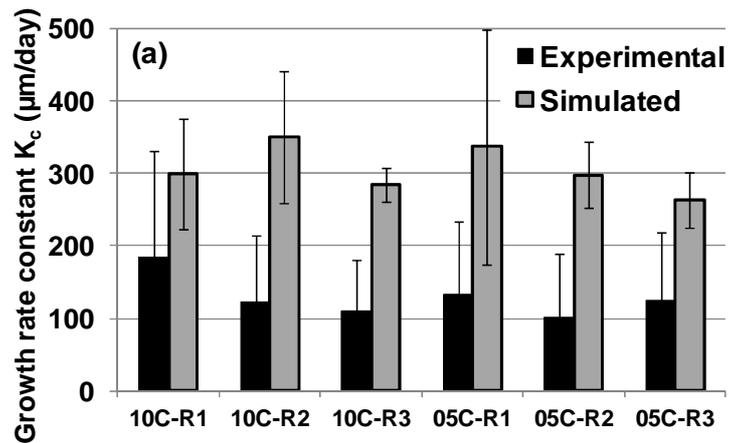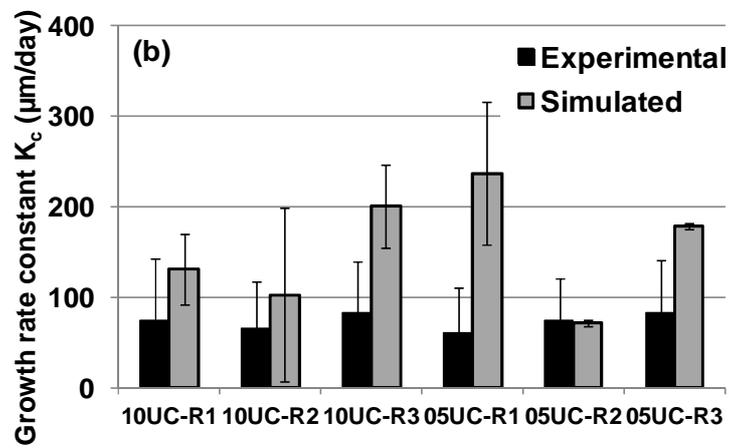
Fig. 11 Comparison between the experimental and the calculated growth rate constants

for carbonated (a) and uncarbonated (b) mortars